Proc. NIPR Symp. Polar Meteorol. Glaciol., 2, 61–69, 1989

A PRELIMINARY ESTIMATE OF INERTIA EFFECTS IN A BULK MODEL OF KATABATIC WIND

Tokio KIKUCHI[1] and Yutaka AGETA[2]

[1]*Faculty of Science, Kochi University, 5–1, Akebono-cho 2-chome, Kochi 780*
[2]*Water Research Institute, Nagoya University, Furo-cho, Chikusa-ku, Nagoya 464–01*

Abstract: Observed sastrugi orientations showed considerable deviation from a bulk theory of katabatic wind in lee sides of troughs in ice sheet undulations of which the wavelength is about 400 km on the Mizuho Plateau, East Antarctica. The effect of the inertia term which may account for the deviations but is often neglected in the equation of motion for katabatic wind is estimated with the perturbation method. A sinusoidally undulating slope with ridges and troughs is assumed for the model calculation instead of an infinite flat slope for the inertia-free model. The calculated results, in a typical inversion, suggest that the inertia term is significant if the wavelength of the undulations is smaller than about 200 km while the effect of the undulations can be neglected if the wavelength is smaller than about 50 km. Observed variability in the wind direction in the lee of the troughs may be accounted for by the effect of the inversion height which enhances the inertia effect.

1. Introduction

On an Antarctic ice sheet slope, where radiative cooling takes place, an inclined inversion layer is formed and a katabatic wind is generated. Knowledge of the windfield on the Antarctic Continent has increased since the early estimate by MATHER and MILLER (1967) based on records of sastrugi orientations obtained during oversnow traverses. Recent theoretical studies by PARISH and BROMWICH (1986, 1987), based on the bulk model by BALL (1956), indicate that the windfield is somewhat different from that of the earlier guess; the simulated pattern shows strong spatial variability with the airflow concentrated into several zones near the coastal margin.

The spatial variability in the katabatic wind seems to be important in many respects. For example, TAKAHASHI (1988) suggested that one of the causes of bare ice fields on the ice sheet is the horizontal divergence in drifting snow transport rate, which is a function of wind velocity. The windfield pattern studies so far have been based on the assumption of negligible inertia terms, and the smallest scale included in the calculation depends mainly on the resolution of the map from which the slope inclination is sampled (PARISH and BROMWICH, 1986).

It seems appropriate to test the validity of the theory in East Queen Maud Land, where Japanese Antarctic Research Expeditions (JARE) are carried out, and check the effect of topographical detail on the windfield through the inertia term which has been omitted from the equation of motion in current theories.

2. Windfield Patterns: Theoretical and Observed

Figure 1 shows the theoretical (thin dashed arrows) and observed (bold and open arrows) windfield patterns derived from the bulk theory and from the sastrugi orientations (FUJIWARA, 1964; FUJIWARA and ENDO, 1971; WATANABE, 1978; OHMAE, 1984; AGETA *et al.*, 1989; and other unpublished data), respectively, in a region where oversnow traverses were carried out by JARE. The bold arrows in Fig. 1 are drawn with consideration to continuity in the data of erosional surface relief (sastrugi) whereas the open ones are drawn for other significant orientations wherever they are found. Another windfield pattern which embodies the depositional system is obtained but is not presented here. Figure 1 is essentially a magnification of Fig. 3 of PARISH and BROMWICH (1987) though the calculation and the data compilation are carried out separately.

Although the theoretical windfield pattern for the katabatic winds which dominate in winter appears to coincide well with most of the observed sastrugi orientations which represent the average wind direction in winter (WATANABE, 1978), there are considerable discrepancies between theory and observations. There is a tendency of the winds to deviate counterclockwise, parallel to the contour lines or to upslope direction on the lee sides of the ice sheet troughts on a slope of about 2.5×10^{-3} inclination, (*e.g.*, at about 72°S, 30°E [A in Fig. 1], and 71°S, 38°E [B]). Coexistence of the open arrows and the bold ones in these areas suggests that the 'true' katabatic wind appears only occasionally and that other unknown factors, one of which is possibly the inertia effect, are important on most of the other occasions.

3. Inclusion of the Inertia Term in Ball's Model

The bulk theory of steady katabatic wind over a homogeneous terrain was first presented by BALL (1956) based on considerations similar to the theory of water flows. By choosing the x-coordinate to point in the downslope direction, a pair of equations of motion are obtained for a surface-attached layer of cold air (inversion layer) having

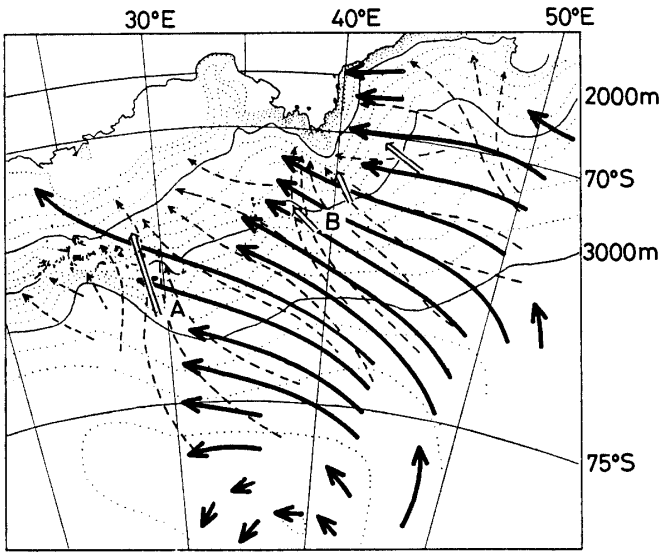

Fig. 1. Windfield pattern in East Queen Maud Land, Antarctica. Bold arrows and open arrows (see text for the difference) represent the estimated pattern from the sastrugi orientations which were observed during the oversnow traverses. Thin arrows with dashed lines represent the wind directions calculated from the bulk model, eqs. (3) and (4). See text for marks A and B.

equal depth along the slope:

$$0=F+fv-(k/H)Vu \tag{1}$$

$$0=F-fu-(k/H)Vv\,, \tag{2}$$

where F is the katabatic force given by $-g(\Delta T/T)\,(\partial h/\partial x)$, g being the gravity acceleration, ΔT the difference in temperature between the inversion layer and the air above, T the free air temperature and h the height of the ice sheet surface. Other notations are: f the Coriolis parameter, k the frictional constant, H the inversion layer depth, and u and v are x and y components of the wind velocity $V=(u^2+v^2)^{1/2}$. The synoptic pressure gradient in the free atmosphere is assumed to be negligible. BALL (1956; see also SCHWERDTFEGER, 1984) shows that eqs. (1) and (2) can be solved for the wind speed and direction γ,

$$V=(HF/k)^{1/2}\cos^{1/2}\gamma=-(F/f)\sin\gamma \tag{3}$$

$$\gamma=\cos^{-1}\{(1+J^2)^{1/2}-J\}\,, \tag{4}$$

where $J=Hf^2/2kF$.

A first step forward to the inclusion of undulations of terrain is to add a small perturbation to the slope. Figure 2 illustrates the model slope under consideration together with BALL's original configuration for comparison. The equations of motion become:

$$v(\partial u/\partial y)=F_x+fv-(k/H)Vu \tag{5}$$

$$v(\partial v/\partial y)=F_y-fu-(k/H)Vv\,. \tag{6}$$

If we put $F_x=F_0=$const., $u=u_0+u'$ and $v=v_0+v'$, and assuming that F_0, u_0 and v_0 satisfy eqs. (1) and (2), then

$$v_0\partial u'/\partial y=\quad +fv'-(k/H)V_0u' \tag{7}$$

$$v_0\partial v'/\partial y=F_y-fu'-(k/H)V_0v'\,, \tag{8}$$

where $V_0=(u_0^2+v_0^2)^{1/2}$ is substituted for V and is assumed to be constant in order that the equations are linearized.

Now, an assumption is made that the katabatic force in the transverse direction

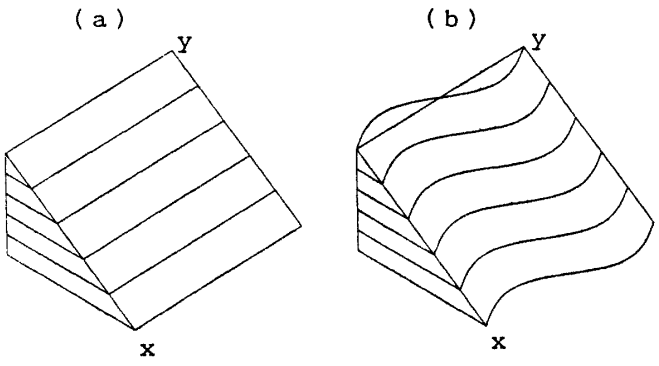

Fig. 2. A schematic representation of the model terrain and the coordinate system. (a) Original bulk model with no undulation (BALL, 1956); (b) present model with a sinusoidal undulation on the terrain.

F_y is represented by

$$F_y=F_1 \cos \kappa y\,, \tag{9}$$

where F_1 and κ are determined from the amplitude D_x and wavelength L of the perturbation as $\kappa=2\pi/L$ and $F_1=(g/T)\Delta T(\partial h/\partial x)D_x\kappa$. Then, a possible solution for u' and v' becomes:

$$\begin{aligned} u'&=u_1 \cos (\kappa y-\alpha) \\ v'&=v_1 \cos (\kappa y-\beta)\,. \end{aligned} \tag{10}$$

One aspect overlooked in the above considerations may be that the equation of continuity is not included in the model; it should be kept in mind that eq. (10) does not satisfy the continuity equation $\partial u/\partial x+\partial v/\partial y=0$. But, it seems that the present simplified system is at least useful it we restrict discussions to the inertia term only.

4. Results and Discussions

A solution of eqs. (7) and (8) for u_1, v_1, α and β is given as follows (see Appendix).

$$u_1=-(f/K_2)v_1 \tag{11}$$

$$v_1=(F_1/K_2)/(K_4 \sin \beta \cos \delta+K_3 \cos \beta \sin \delta) \tag{12}$$

$$\beta=\tan^{-1}(K_4/K_3 \tan \delta) \tag{13}$$

$$\alpha=\beta-\delta-(\pi/2)\,, \tag{14}$$

where

$$K_2=\{(kV/H)^2+(v_0\kappa)^2\}^{1/2} \tag{15}$$

$$\delta=\tan^{-1}(kV_0/Hv_0\kappa) \tag{16}$$

$$K_3=1+(f/K_2)^2 \tag{17}$$

$$K_4=1-(f/K_2)^2\,. \tag{18}$$

Figure 3 shows some of the examples obtained through eqs. (11) -(14) by changing the parameters L and D_x. The inclination of the original undisturbed slope is fixed at 3×10^{-3}, which is a typical value for the Antarctic ice sheet being considered. The strength and height of the inversion, ΔT and H, are taken at -10 K and 200 m, respectively (KAWAGUCHI *et al.*, 1982). The frictional constant k is assumed to be 0.005 after PARISH and BROMWICH (1986, 1987).

In Fig. 3(b) and (c), the shaded areas represent those in which contour-parallel or upslope winds are observed. Even though upslope winds are made possible by including the inertia term, the area is restricted to the immediate lee of the trough. The observed contour-parallel or upslope winds in Fig. 1 extend to the ice ridges. It seems that there are difficulties in explaining the observed windfield by the present model.

The windfield pattern in Fig. 3(a) in a horizontal wavelength L of 500 km shows a

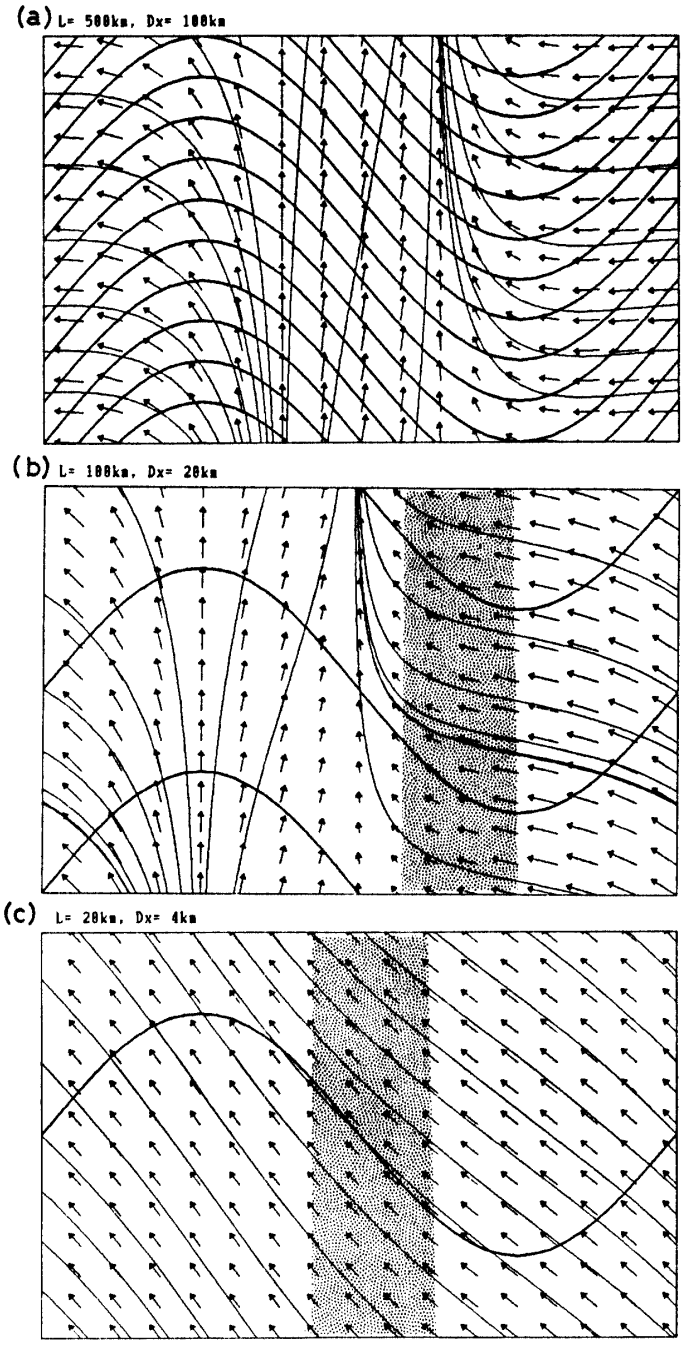

Fig. 3. Examples of the calculated windfield which are represented by vector arrows and stream lines. Bold lines are contours of terrain and are drawn every 100 m elevation. The slope inclination $\partial h/\partial x=0.003$, the inversion height $H=200$ m, the inversion strength $\Delta T=-10$ K and the frictional constant $k=0.005$. (a) The horizontal wavelength $L=500$ km and amplitude $D_x=100$ km, (b) $L=100$ km and $D_x=20$ km, and (c) $L=20$ km and $D_x=4$ km. The shaded areas in (b) and (c) represent up-slope wind regions.

confluence zone in the lee of the trough and a difluence zone on the ridge. This feature of confluence/difluence pattern has already been noted by PARISH and BROMWICH (1987). A windfield pattern from BALL's original model is also drawn, for comparison, by using the local values of the slope parameters, but it is not shown here because it is almost identical to Fig. 3(a).

The pattern in Fig. 3(c), $L=20$ km, does not appear to be disturbed by the surface undulation, and little confluence/difluence pattern is observed. The difference in the pattern with the scale is reasonable since the inertia scale, which is almost constant, will become larger than the topographic scale as the wavelength becomes smaller.

Besides the leeward shift of the windfield, which is a natural result of the inertia effect, a peculiar feature appears in the intermediate scale $L=100$ km, Fig. 3(b); it appears that the confluence/difluence effect of the undulating terrain is somewhat intensified. Nevertheless, it is questionable that this type of windfield can appear in nature, as long as the equation of continuity is neglected. The confluence will either accelerate the katabatic wind, or make the inversion height infinitely large. However, on second thought, it may be possible to omit continuity considerations if an entrainment process is present at the upper boundary of the inversion layer. It seems that a more refined model is required to describe the katabatic wind on this intermediate scale.

The effect of the topographic scale is also seen in Fig. 4, which shows the disturbance amplitude of wind velocity $V'=(u_1^2+v_1^2)^{1/2}$ and the maximum difference between the wind direction by the present model and that derived from BALL's model with local parameters, $\Delta\gamma$, as functions of the wavelength. The amplitude of the wave in contours is fixed at a tenth of the wave length. On a small scale, less than about 50 km, V' becomes small; thus the undulation in the terrain can be neglected. On the other hand, the wind seems to be determined solely by the local parameters on scales larger than about 200 km since $\Delta\gamma$ becomes small in this region. There is an intermediate region, 50–200 km, in which neither the undulation nor the inertia term can be neglected.

Figure 5 shows the effect of other parameters ΔT and H. In Fig. 5(a) the temperature difference ΔT is doubled, while the inversion height H is doubled in (b). The undisturbed wind velocity V_0 increased from 5.8 m/s in the original to 8.9 m/s and 7.1 m/s in (a) and (b), respectively. Apparently, the inertia effect is enhanced in (b). The wind direction does not change significantly on the ridge or up-wind of the trough, while its change is most significant in the lee of the trough. This effect of the difference in structure of katabatic winds may account for the observed coexistence of bold and open arrows at A and B in Fig. 1.

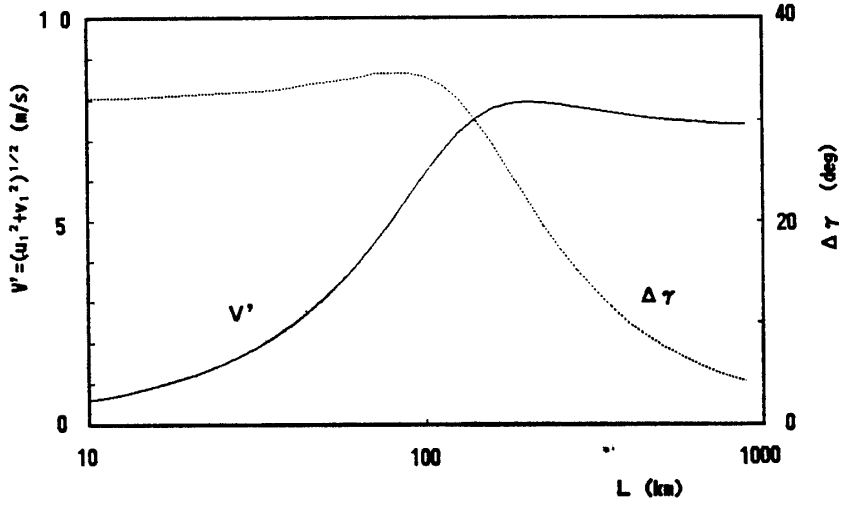

Fig. 4. The perturbation amplitude in the wind speed V' and the difference in the wind direction from the original bulk model with local parameters $\Delta\gamma$ as functions of contour line wavelengths.

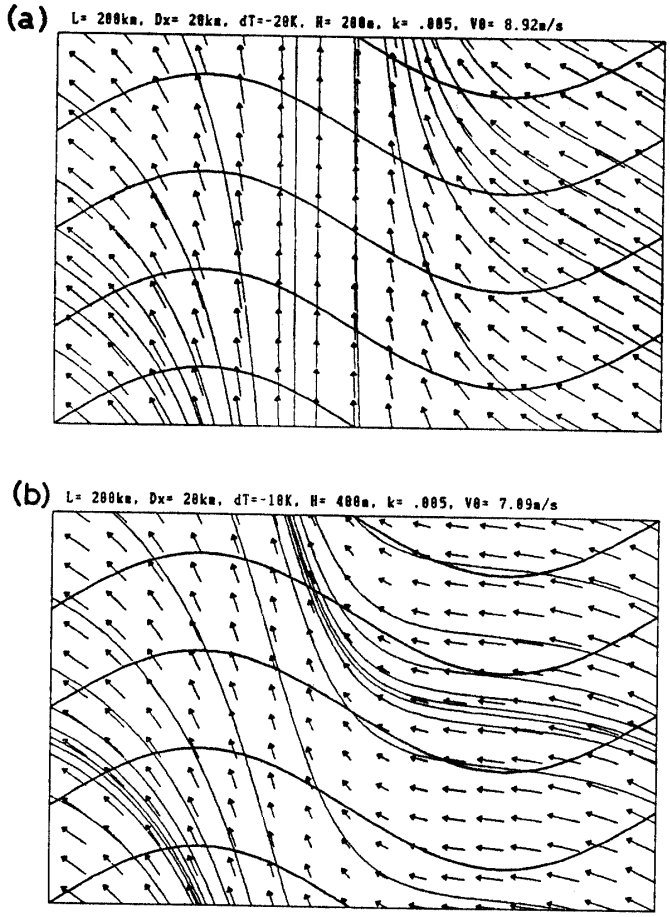

Fig. 5. Effect of katabatic wind structure parameters ΔT and H. ΔT and H are doubled in (a) and (b), respectively. Other symbols are the same as in Fig. 3.

5. Conclusion

A preliminary estimate is made of the effect of the inertia term in a bulk model of the katabatic wind by applying the perturbation method to undulating slopes with ridges and troughs and by varying the wavelength of the undulations. Small scale undulations of the surface terrain can be neglected in the calculation of wind velocity as long as the scale is smaller than about 50 km. The local values of slope and inversion parameters determine the wind velocity if the wavelength of the undulations is larger than about 200 km. There are intermediate scales on which neither the effect of undualtion nor that of inertia can be neglected. The observed variability in wind direction in the lee of the troughs may be accounted for by the effect of the inversion height, which enhances the intertia effect. A more refined model is required for further discussion because the present model is insufficient, in that equation of continuity is omitted.

Observational studies in the Antarctic katabatic wind zone suggest that there is considerable coupling between the boundary layer and the upper atmosphere by diurnal convection in summer (SORBJAN *et al.*, 1986; KIKUCHI *et al.*, 1988). Gravity wave activity which has been observed throughout the year (NEFF, 1981; KIKUCHI, 1988) may be another indication that the boundary layer is not completely separated from the upper atmosphere. In this respect, the simplified bulk theory seems to be inadequate

for a detailed study of winds over a complex terrain. The three-dimensional primitive equation model developed by WAIGHT (1987, see PARISH, 1988) would be useful in further studies.

Acknowledgments

Dr. H. NARITA, Dr. K. SATOW, Dr. J. INOUE, Dr. T. OHATA and Dr. K. KAWADA kindly provided their unpublished data of sastrugi orientations. This study was supported by a grant from the Ministry of Education, Science and Culture, Japan (Nos. 61302023 and 62740238).

References

AGETA, Y., KAMIYAMA, K., OKUHIRA, F. and FUJII, Y. (1989): Geomorphological and glaciological aspects around the highest dome in Queen Maud Land, East Antarctica. Proc. NIPR Symp. Polar Meteorol. Glaciol., **2**, 88–96.

BALL, F. K. (1956): The theory of strong katabatic winds. Aust. J. Phys., **9**, 373–386.

FUJIWARA, K. (1964): Preliminary report on the morphology of the inland ice sheet of the Mizuho Plateau, East Antarctica. Nankyoku Shiryô (Antarct. Rec.), **23**, 1–11.

FUJIWARA, K. and ENDO, Y. (1971): Preliminary report of glaciological studies. JARE Sci. Rep., Spec. Issue, **2**, 68–109.

KAWAGUCHI, S., KOBAYASHI, S., ISHIKAWA, N. and OHATA, T. (1982): Aerological sounding of the surface boundary layer at Mizuho Station, East Antacrtica. Mem. Natl Inst. Polar Res., Spec. Issue, **24**, 77–86.

KIKUCHI, T. (1988): A case study of a wave-like cloud and gravity wave in the lower troposphere in Mizuho Plateau, Antarctica. Boundary-Layer Meteorol., **43**, 403–409.

KIKUCHI, T., AGETA, Y., OKUHIRA, F. and SHIMAMOTO, T. (1988): Climate and weather at the Advance Camp in East Queen Maud Land, Antarctica. Bull. Glacier Res., **6**, 17–25.

MATHER, K. B. and MILLER, G. S. (1967): Notes on topographic factors affecting the surface wind in Antarctica, with special reference to katabatic winds. Univ. Alaska, Tech. Rep., UAGA-**189**, 125 p.

NEFF, W. D. (1981): An observational and numerical study of the atmospheric boundary layer overlying the East Antarctic ice sheet. NOAA Technical Memorandum ERL WPL-**67**, 272 p.

OHMAE, H. (1984): Direction of long axis of a sastrugi. JARE Data Rep., **94** (Glaciol. 10), 114–116.

PARISH, T. R. (1988): Surface winds over the Antarctic continent; A review. Rev. Geophys., **26**, 169–180.

PARISH, T. R. and BROMWICH, D. H. (1986): The inversion wind pattern over West Antarctica. Mon. Weather Rev., **114**, 849–860.

PARISH, T. R. and BROMWICH, D. H. (1987): The surface windfield over the Antarctic ice sheets. Nature, **328**, 51–54.

SCHWERDTFEGER, W. (1984): Weather and Climate of the Antarctic. Amsterdam, Elsevier, 261 p.

SORBJAN, Z., KODAMA, Y. and WENDLER, G. (1986): Observational study of the atmospheric boundary layer over Antarctica. J. Climate Appl. Meteorol., **25**, 641–651.

TAKAHASHI, S. (1988): A bare ice field in East Queen Maud Land, Antarctica, caused by horizontal divergence of drifting snow. Ann. Glaciol., **11**, 156–160.

WAIGHT, K. T. (1987): The dynamics of Antarctic katabatic winds. Ph. D. Thesis, Dep. Atmos. Sci., Univ. Wyoming, Laramie, 172 p.

WATANABE, O. (1978): Distribution of surface features of snow cover in Mizuho Plateau. Mem. Natl Inst. Polar Res., Spec. Issue, **7**, 44–62.

(Received March 4, 1988; Revised manuscript received September 27, 1988)

Appendix. Derivation of Eqs. (11)–(14)

Equations (11) through (14) can be obtained as follows: first, substitute eqs. (9) and (10) into eqs. (7) and (8),

$$-v_0u_1\kappa \sin(\kappa y-\alpha)= -fv_1 \cos(\kappa y-\beta)-K_1u_1 \cos(\kappa y-\alpha) \tag{A1}$$

$$-v_0v_1\kappa \sin(\kappa y-\beta)=F_1 \cos \kappa y-fu_1 \cos(\kappa y-\alpha)-K_1v_1 \cos(\kappa y-\beta) \tag{A2}$$

where $K_1=kV_0/H$. With a little trigonometric algebra eq. (A1) becomes

$$\begin{aligned}&\cos \kappa y(fv_1 \cos \beta-K_1u_1 \cos \alpha-v_0u_1\kappa \sin \alpha)\\ &+\sin \kappa y(fv_1 \sin \beta-K_1u_1 \sin \alpha+v_0u_1\kappa \cos \alpha)=0\end{aligned} \tag{A3}$$

The two coefficients of the sinusoidal functions closed in parentheses must be zero because eq. (A3) must be valid independent of y. Then, with eqs. (15) and (16),

$$fv_1 \cos \beta-K_2u_1 \sin(\alpha+\delta)=0 \tag{A4}$$

$$fv_1 \sin \beta+K_2u_1 \cos(\alpha+\delta)=0 \tag{A5}$$

Now calculate (A4)$\times\sin\beta$+(A5)$\times\cos\beta$:

$$\sin(\alpha+\delta) \sin \beta+\cos(\alpha+\delta) \cos \beta=0$$

or,

$$\cos(\beta-\alpha-\delta)=0$$

therefore,

$$\beta-\alpha-\delta=\pm\pi/2\,. \tag{A6}$$

Next, it follows from (A4)$\times\cos\beta$+(A5)$\times\sin\beta$:

$$fv_1+K_2u_1 \sin(\beta-\alpha-\delta)=0$$

thus,

$$\sin(\beta-\alpha-\delta)=-fv_1/K_2u_1 \tag{A7}$$

Since $f<0$ in the southern hemisphere and $K_2>0$, the right hand side of eq. (A7) becomes positive, assuming u_1, $v_1>0$. Then, from eq. (A6),

$$\sin(\beta-\alpha-\delta)=1\,.$$

Therefore, eqs. (11) and (14) are obtained.

It also follows from (A2) that

$$F_1-fu_1 \cos \alpha-K_2v_1 \sin(\beta+\delta)=0 \tag{A8}$$

$$fu_1 \sin \alpha-K_2v_1 \cos(\beta+\delta)=0 \tag{A9}$$

with a similar process as that from eq. (A1) to eqs. (A4) and (A5). Equations (12) and (13) follow by substituting eqs. (11) and (14) into (A8) and (A9).